Fernández-Sarría, A.; López- Cortés, I.; Marti-Gavila, J.; Estornell Cremades, J. (2022). Estimation of Walnut Structure Parameters Using Terrestrial Photogrammetry Based on Structure-from-Motion (SfM). Journal of the Indian Society of Remote Sensing. 50(10):1931-1944. https://doi.org/10.1007/s12524-022-01576-x

Estimation of walnut structure parameters using terrestrial photogrammetry based on structure-from-motion (SfM)

Abstract

Remote sensing techniques are increasingly used for crop monitoring to improve the profitability of plantations. These studies are mainly based on spectral information recorded by satellites or unmanned aerial vehicles (UAVs). However, the development of Earth Observation Systems (EOS) capable of retrieving 3D point clouds at an affordable cost enables the possibility of exploring new approaches in agriculture. In this context, more research is required to analyze the capability of 3D data for inventory, management and prediction of inputs (water, fertilizers and pesticides) and outputs (production, biomass) of fruit plantations. To do this, the complete representation of each tree contributes to extract the main geometric parametersThe objective of this work is to obtain regression models to estimate total height (Ht), crown height (Hc), stem diameter (Ds), crown diameter (Dc), stem volume (Vs) and crown volume (Vc) from 45 walnut specimens. For this, 3D models were computed for these trees by applying ground-based Structure from Motion (SfM). A circular photogrammetric survey of each tree was carried out using a standard digital camera and three-dimensional point clouds were retrieved for each tree. From these data, the tree parameters were computed. Linear regression models were obtained to estimate Ht, Hc, Ds, Dc, Vs and Vc, with R^2 values between 0.89 to 0.99. The results showed accurate fits between field parameters and those derived from 3D point clouds retrieved from SfM technique, indicating the applicability of this cost-effective method to model walnut trees and to extract their accurate parameters without costly field campaigns.

Keywords Structure from motion (SfM); automated photogrammetry; walnut tree; precision agriculture; geometrical parameters.

Introduction

Agriculture is subjected to the development of advanced management techniques that maximize crop yields while minimizing economic and environmental costs. Access to updated, accurate, and cost-effective data of individual trees plays an important role when analyzing pattern variations within a plot and suitable decision-making in agricultural management practices. In this sense, mapping individual fruit trees based on EOS data is crucial to extract structure parameters (Tagarakis et al. 2018; Jiménez-Brenes et al. 2017; Gené-Mola et al. 2020; Gil et al. 2014; Walklate et al. 2002).Remote sensing data have been widely used in agriculture in recent decades (Miao et al. 2009; Xie et al. 2019). These applications are based on the processing of reflected or emitted electromagnetic energy using specific wavelengths. Additionally, the development of advanced systems to register 3D point clouds enables exploring new approaches for precision horticulture. Previous research has established that LiDAR (Light Detection And Ranging) data can be used to estimate aboveground biomass and volume (Sheridan et al. 2015); forest structural attributes (Valbuena et al. 2016; Zhang et al. 2017); map individual trees (Stereńczak et al. 2020) and predict forest canopy fuel parameters (Maltamo et al. 2020). Allometric equations for calculating biomass or volume of forest trees are commonly used based on basic geometric parameters (Schlaegel et al. 1984; Jenkins et al. 2004; Xing et al. 2019). However, there has been little discussion about the relationships among total and crown biomass and geometric parameters of fruit trees. While forest trees concentrate their volume and biomass in their trunks, this does not occur in fruit trees, as these are mainly distributed throughout their crowns (Velázquez-Martí et al. 2014). Management practices applied on these trees can explain the difficulty in defining these allometric equations. In addition, it is challenging, highly laborious, and complex to measure and characterize the crowns of fruit trees from measurements taken in the field using non-destructive methods, especially for irregular and large trees. Therefore, further research is required to analyze the capability of terrestrial remote sensing systems for studying the crown structure of fruit trees and analyzing their potential in agricultural management. This information could be used to analyze their applicability for estimating pruning and crown biomass, fruit production, irrigation necessities, and pesticides to be applied in farms. Crown biomass data estimated from tree parameters retrieved using 3D data can also be applied to quantify carbon sequestration in agricultural systems. These applications reveal the potential of altimetry systems in agriculture such as LiDAR or based on photogrammetric techniques to obtain 3D cloud points.

According to the platform used, LiDAR systems can be classified into ground-based, airborne, and satellite systems. For the first group, terrestrial laser scanner (TLS) and mobile terrestrial laser scanners (MTLS) are the most common systems applied in agriculture (Walklate et al. 2002; Moorthy et al, 2011; Sanz et al. 2018). For TLS systems, a dense set of 3D points with millimeter detail (Liang et al. 2016) is measured to retrieve structural tree parameters (Moorthy et al. 2011; Estornell et al. 2017; Fernández-Sarría et al. 2019). Previous studies based on TLS data reported the capability of these systems to estimate the crown volume of walnut trees (Estornell et al. 2017), pruning biomass, and plant area indexes for olive trees (Moorthy et al. 2011; Fernández-Sarría et al. 2019) which can replace laborious ground-based methods. Nevertheless, this system is not efficient in large plots and presents several drawbacks: the cost of instrumentation; the need for several stations to completely scan trees and avoid occlusions; and the need for large sets of data requiring significant computing resources. Tree biomass was estimated in forestry plots using TLS computing, firstly, generating architectural tree models, and, secondly, calculating their volumes (Calders et al. 2015; Gonzalez de Tanago et al. 2018).

MTLS systems are mounted on moving vehicles integrating some sensors that provide position and movement vectors (GNSS and IMU) in addition to those that register target data (camera, laser scanner, thermal sensors, etc.). Applied in farming, multiple vertical scans can be registered laterally along the rows of plots to generate 3D point clouds (Escolà et al. 2017). These LiDAR systems enable registering most of the trees in a plot in a reasonable period of time. MTLS systems show great potential for estimating canopy volumes and leaf area index (LAI) measurements (Arnó et al. 2013; Auat Cheein et al. 2015). Low cost systems based on 2D LiDAR sensors are commonly used in agriculture (Palacín et al. 2007; Ehlert et al. 2010). These systems are based on the emission of a laser beam in a Y, Z plane perpendicular to the movement direction from a sensor (LMS-200, ±15 mm accuracy) mounted on a tractor. Points with polar coordinates are obtained from the sensor position. The movement of the platform in the X direction enables obtaining points with a series of profiles or sections of the crops with information on one side that is completed with a similar measurement on the other side (Arnó et al. 2013). Nevertheless, several researchers report that to simplify the registering process and the estimation of some structural variables, LiDAR data was registered only from one side and this can generate some uncertainties related to the influence of orientation on each side of the tree rows (Arnó et al. 2015). Other studies reported the limitation of these systems for registering data inside the crowns (Escolà et al. 2017). The distance to the target can be another limiting factor reducing vertical sampling resolution (Escolà et al. 2017). This technology can

be used in farms where distances among tree rows are wide enough for mobile devices, but it cannot be used in small plots with densely planted trees and without a regular distribution frame.

Several researchers propose the integrated application of MTLS and SLAM algorithms (Simultaneous Localization and Mapping Algorithm). This technique uses the positional and movement parameters of the equipment to produce a map, in the form of 3D point clouds (Cadena et al. 2016).

Pierzchala et al. (2018) have applied this technique to forest areas using a Velodyne VLP 16 LiDAR sensor. Dong et al. (2017) have recurrently applied SLAM in forest and agricultural environments to spatio-temporally model vegetation, characterizing changes in these dynamic spaces. This leads to the concept of 4D reconstruction, possible after calculating 3D models for each crop row in each time session. The combination of all of them allows 4D modelling, which is of great interest in vegetation evolution.

Airborne LiDAR systems include sensors mounted on aircrafts, helicopters, and unmanned aerial vehicles (UAV). Aircraft sensors enable measuring large areas by registering all the trees within a plot and including those planted very close together and so difficult to measure by other LiDAR techniques. These systems show a remarkable potential to extract individual trees (Hadas et al. 2017), estimate structural parameters (Popescu et al. 2007; Kankare et al. 2013), and other parameters related to management operations, such as pruning (Estornell et al. 2015). As drawbacks, aircraft systems tend to underestimate tree heights (Lefsky et al. 2002; Bork et al. 2007) and insufficient data are recorded from the lower parts of the canopy to analyze its structure (Van der Zande et al. 2006; Estornell et al. 2015; Estornell et al. 2018) . In addition, the flight costs are significant, and the data of neighboring plots are also unnecessarily registered. UAV systems equipped by LiDAR sensors offer a more efficient solution by registering the data of selected plots at lower costs. Additionally, since the flight height is lower than aircraft systems, it is possible to register tree canopies in great detail, extracting stem and branch geometry. Some studies reported that accurate definitions of stems from UAVs can be achieved in forest environments (Brede et al. 2019). Dalla et al. (2020) conclude that stems and branches with diameters greater than 30 cm showed good correlations between TLS and UAV-LiDAR data, with decreasing accuracy for young trees. Wieser et al. (2017) demonstrated that the accuracy and geometric definition of cylindrically shaped stems in forest species depends on their diameters, obtaining DBH differences of 9% for diameters between 20 and 30 cm and more accurate results for DBH larger than 40 cm. But the stems of fruit trees, which are usually thinner than forest trees, often are leaning, they are not completely cylindrical, having irregularities due to their growth or pruning and rarely reach the height at which DBH is generally measured (1.30 m). These

particularities make that further research is needed to analyze the potential of LiDAR data acquired by drones and to test their applicability for fruit trees. Finally, for satellite systems Geoscience Laser Altimeter System (GLAS) on board ICESat-1 and 2 satellites were launched to obtain vegetation information among other applications (Wang et al. 2011; Neuenschwander et al. 2019).

In addition to using LiDAR systems to obtain 3D data, algorithms based on photogrammetric techniques and computer vision have enabled the development of cost effective solutions for extracting three-dimensional information of terrestrial targets, either through cameras on board in UAVs or with terrestrial cameras (Goesele et al. 2007; Snavely et al. 2008). Among all the existing photogrammetric processes and algorithms, structure from motion (SfM) is a technique in which, through the automatic identification of homologous points in several conventional and uncalibrated photographic images, the position and orientation of the camera and each image can be calculated. From this information and considering the overlap among images it is possible to reconstruct the scenes in 3D and so create, almost automatically, 3D models of any object or surface. Since the intrinsic parameters of the camera are automatically estimated during the geometric reconstruction phase, no prior calibration of the camera is required (Jay et al. 2015). This processing can be complemented with multi-view stereo (MVS) to obtain three-dimensional clouds with high point density.

The processing flow basically consists of five phases: (i) feature detection and establishment of correspondence between points in all images taken for defining sensor parameters and relative position (Chang et al. 2017). The aim is to automatically detect the key points common to several photographs using invariant scaling, translation, rotation, and radiometry algorithms such as Scale Invariant Feature Transform (SIFT) (Lowe et al. 2004); (ii) reconstruction of the geometry of the photographic shot by applying triangulation and determining the position of the key points in space from at least two different images in which each point appears and logging the positions and orientations of the camera in each photograph; (iii) block adjustment of the group of rays that join the projections and physical points in such a way that the reprojection error is as low as possible and thus obtaining a cloud of linking points; (iv) application of MVS algorithms that enable increasing density of link point clouds (or scattered cloud), starting from the geometry of the shot and link points to obtain a high density of points with relative X, Y, Z coordinates; (v) although this last step is not necessary, the model can be provided with scale, absolute coordinates, and metrics, and points with known coordinates can be located (using GNSS). A high-density 3D point cloud is therefore obtained, and the same algorithms used for LiDAR data can be applied on those data to obtain

projected areas, crown and stem volumes, canopy and tree heights, information of stem and strata tree and among others.

The potential of the SfM technique with cameras on board in UAVs has been tested in forest ecosystems (Wallace et al. 2016, Guerra-Hernández et al. 2018). Single tree inventory variables were estimated using these techniques (Miller et al. 2015; De Eugenio et al. 2018). In agriculture, the geometric characteristics of various crops were obtained (Jay et al. 2015; Chang et al. 2017;) and this enabled an estimation of plant biomass (Torres-Sánchez et al. 2018) and a monitoring of its phenological evolution (Dong et al. 2017) even in semi-arid environments (Cunliffe et al. 2016). The advantages of SfM techniques are that they enable estimating at low-cost tree parameters with great spatial detail (Zarco-Tejada et al. 2014; Díaz-Varela et al. 2015) and they can be used for individual and selected parcels The greater flexibility in the acquisition process enables obtaining repetitive data in a short period of time (Gómez-Candón et al. 2014). All these advantages mean that this technology has great potential to be applied in horticulture. However, these systems can provide valuable information for extracting tree and height modelling, the capability for defining stems and 3D crown structure require further analysis. In fact, only 3D points of the outermost canopies are retrieved. Another constraint of these systems is that the effect of shadows on the images makes the photogrammetric processes more complex. For measuring the lateral sides of trees, it is important to analyze the effect of angle observation and so avoid the problems inherent in a zenithal shot. In addition, these systems require UAVs, whose costs are quite variable, and required qualified staff to pilot them.

Terrestrial photogrammetry based on SfM can offer an interesting alternative. These low-cost systems are based on the use of standard digital cameras, as in the case of UAVs. However, one of the advantages is that the user only has to take images around the tree and this process is quick. In addition, this observation system is flexible and can register data from the highest and lowest parts of the canopies and stems of the trees. Therefore, it is worthwhile analyzing the performance of these techniques for obtaining the basic parameters of trees.

The aim of this study is to estimate total and crown height, stem and crown diameter and stem and crown volume of walnut trees applying Structure from Motion (SfM) method on terrestrial images taken by a standard digital camera. The species studied is the walnut tree (*Juglans regia L.*), a tree that is increasing popular in Spain, varying from 10,212 ha in 2010 to 15,204 ha in 2019 (Ministerio de Agricultura, Pesca y Alimentación, 2019). It is evaluated correspondence between standard field methods

and this photogrammetric technique to estimate both crown and stem features (height, diameter and volume).

Materials and methods

Field data

A set of 45 walnut trees covering a wide and continuous range of values in terms of crown and stem diameter (Table 1) was sampled in December 2017 - January 2018. The sample trees are located in two irrigated plots in the municipality of Viver (Castellón, Spain) (Fig. 1). The soil has a sandy-loam texture and is calcareous with an isopropyl-n-phenyl carbamate (IPC) of 35. It is deep although it has little organic matter, and is reddish-brown in color. The average rainfall in the area is 556 mm, and the relative humidity is 60.14%. The lowest and highest average monthly temperatures and the annual average in recent years (*http://agroclimap.aemet.es*) have been 7.9˚ C, 22.8˚ C and 14.6˚ C respectively. The reference evapotranspiration (ET_0) is 116.51 mm (Hargreaves 1994).

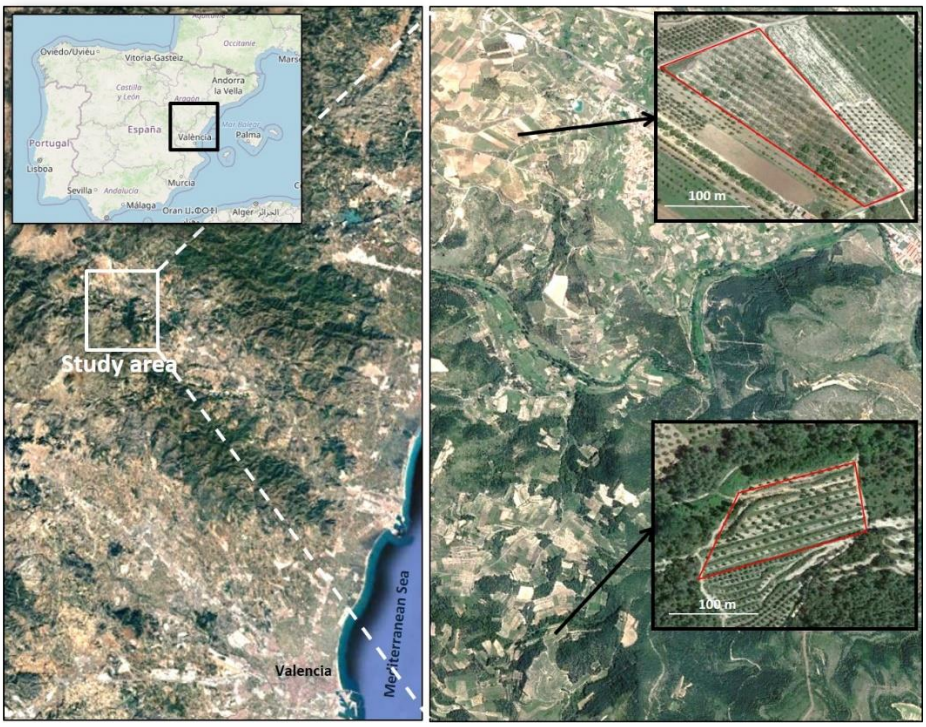

Fig. 1. Study area showing the location of the two irrigated plots (images from Open Street Map and Google Earth).

The specimens used in the study are grafted on stems of the same species after two years of seedling, which is the majority pattern in limestone areas, where the two plots are located. The adult specimens are a maximum age of 28 years old, and although this plantation was originally dry, controlled deficit irrigation was installed about 18 years ago. The growth of the walnut trees is considered to be very adequate for the age of the plantation, taking into account that pruning has always been done by carefully eliminating branches to allow good aeration and a high photosynthetic efficiency. The following parameters were measured for the 45 trees: total height (Ht) was measured from three locations, using a pole to measure the highest branch of a tree. Stem height (Hs) was measured from the ground to the first bifurcation using a tape. Stem diameter was (Ds) measured at 0.60 m from the ground using a pi tape. Crown height (Hc) was calculated from the previous data (Ht-Hs). Since trees were sampled without leaves, the crown diameters were not measured in the field. To obtain the crown diameters (Dc) of each tree, an orthophoto of July of 2017 (Orthophoto 2017 CC BY 4.0 © Institut Cartogràfic Valencià, Generalitat) with a pixel size of 0.25 × 0.25 m and a false color composition (IR, R, G) were used. Four measurements per tree in the directions N-S, W-E, NW-SE, and NE-SW were then taken and their average value was calculated. In the orthophoto, walnut trees were leafy, and crown shapes and their diameters could be identified more accurately than when leafless. For leafless trees, it was difficult to identify the crown boundary, especially for large specimens. Crown growing differences between the periods of field campaign and orthophoto can be considered insignificant, since annual pruning was applied after taking images (February 2, 2018). Stem volume (Vs) can be adjusted to that of a cylinder of height and diameter measured manually with a tape. However, this results in a significant loss of accuracy in the volume value. Indeed, of all the measured specimens, only the youngest could have a cylindrical trunk. In the adult specimens, it is common to find that the base of the steam is wider than a few centimeters above in height, and there is a clear non-circular widening in the upper part of the stem, where the branches of stratum 1 of the crown diverge, as can be seen in Fig. 4.

For all these reasons, measurements of the diameters of the stems were taken from the base, every 20 cm in height (stem diameter was invariant at this interval), and finally at the crown (given the irregular shape at this height, two perpendicular measurements were taken and averaged). The stem volume was obtained as the sum of the volumes of cylinders between two successive diameter measurements (base, every 20 cm, and crown). Table 1 shows a high disparity in the stem volumes, a consequence of the different sizes of the walnut trees. Crown volume (Vc) also presents a high disparity for the same reason as the

diameter of the stem. It was calculated using the equation of a paraboloid solid as a surface model by Eq. (1). This solid was used in previous studies (Estornell et al. 2017) and was selected since it is the model that best fits the crown in comparison to hemisphere, cone, and cylinder models.

$$V_c = \frac{1}{2}\,\frac{\pi \cdot D_c^2 \cdot H_c}{4} \quad (1)$$

Where Vc (m^3) is the volume of the paraboloid used to model the crown, Dc (m) the crown diameter, and Hc (m) the crown height.

Table 1 Statistics of walnut parameters measured in field (n = 45). Total height (Ht); crown height (Hc); crown diameter (Dc); stem diameter (Ds); stem volume (Vs); crown volume using a paraboloid shape (Vc).

Statistic	Ht (m)	Hc (m)	Dc (m)	Ds (cm)	Vs (m^3)	Vc (m^3)
μ	5.11	4.20	5.05	17.59	0.042	74.97
σ	1.93	1.83	2.79	8.29	0.041	97.44
Min	2.43	1.67	1.43	7.20	0.005	1.33
Max	9.25	8.33	10.63	33.80	0.160	358.58

Structure from motion methodology

Building a 3D model using SfM requires photographs from different angles around each tree. The systematic capture of a photograph every specified time lapse enables a high overlap between images in such a way that the same point is identifiable in several images. This enables a better reconstruction of the geometry (Jay et al. 2015).

A GoPro Hero4 Black camera was used with a resolution of 12 MP, and images were captured every 0.5 seconds with a wide FOV, 28 mm focal length focus, auto exposure time, and ISO-100. The camera was adapted to the end of a surveying rod extended to a height of two meters. The camera was elevated to about 3.5 meters in height and a continuous and circular capture was made around each tree. For adult trees, an average of 80 photographs were taken with a large overlap. For the young walnut trees, the approximate height of the camera was about 2.5 meters and the average number of photographs per tree

was 70. The time spent to take images around each tree oscillated between 30-60 seconds. It took approximately two and a half hours of field work to take images for the 45 trees.

The photographs were taken on February 2, 2018, with a cloudy sky and hardly wind, in ideal lighting conditions to avoid the strong contrast between sunny and shady areas (Fig. 2). To provide metrics and scale to the models, two orthogonal range poles were used in the XY plane and two more in a vertical direction (Fig. 2, Fig. 3). Subsequently, four distances (one per range pole) were defined in each photograph.

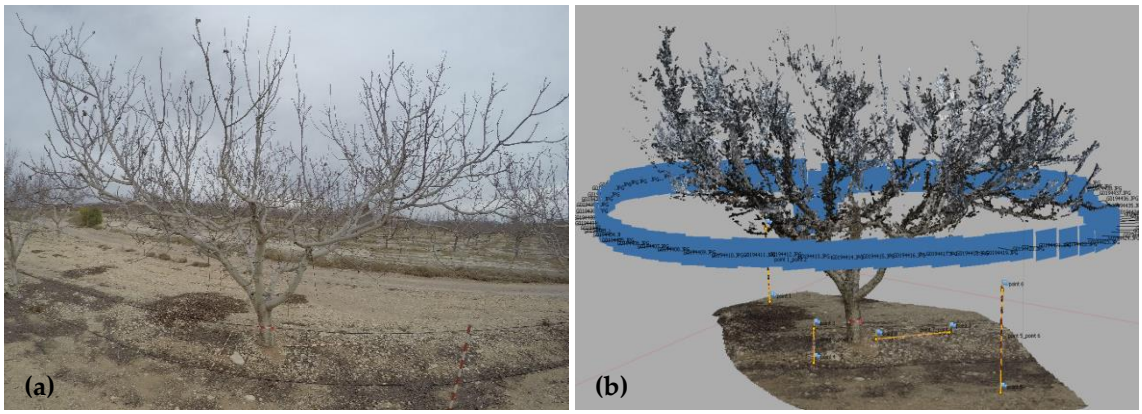

Fig. 2. Photograph of an adult walnut (a) and point cloud created with the position of the photographs and markers that define the four scaling distances (b).

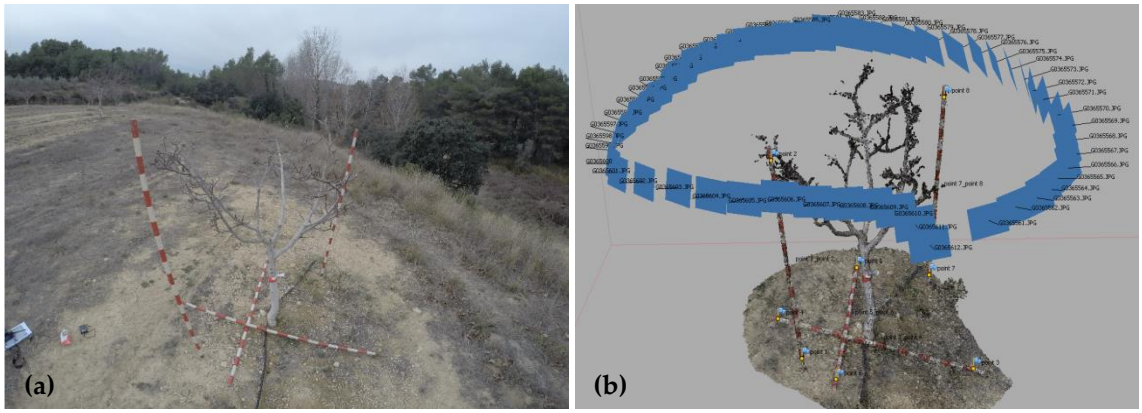

Fig. 3. Photograph of a young walnut (a) and point cloud created with the position of the photographs and markers that define the four scaling distances (b).

SfM processing was performed using Agisoft PhotoScan Professional Edition software (Agisoft LLC) version 1.2.5 build 2735. It is a quasi-automatic process, requiring just the manual localization of

four distances in each image to set the model scale. This software performs several steps: firstly, the images are aligned and the position of the camera and the orientation of each image are identified automatically (Fig. 2 and Fig. 3 show the position of the cameras in the circular movement around each tree). An initial scattered point cloud is created in this step. Secondly, the distances to calibrate geometrically the model in the successive frames are defined. An accuracy of 2 cm is defined by default in the identification of distance measurements, obtaining errors in the bundle adjustment for all the photographs ranging from 0.1 cm to 1.4 cm. Finally, a dense cloud is then created.

As can be seen in Fig. 4, an accurate definition of the geometry of the tree is achieved in both adult and young specimens. The stems are perfectly defined because the surfaces are clearly identifiable in the photographs. In the upper and terminal parts of the branches, their smaller size combined with the slight movement caused by the low wind and the mixing of radiometric levels with the background sky, caused many errors that were necessary to manually clean (Fig. 5 shows an example of the result of the cleaning process). Even so, large errors are still evident, such as duplicities at the ends of some small branches as a consequence of the occultations that can occur between successive images or wind. Moreover, there is less accuracy in the upper parts and further away from the geometric centers of the cameras. The points corresponding to the ground are eliminated and the point clouds are exported in LAS format to apply the three-dimensional data processing algorithms, such as those implemented in Cloudcompare version 2.8 *(www.cloudcompare.org).*

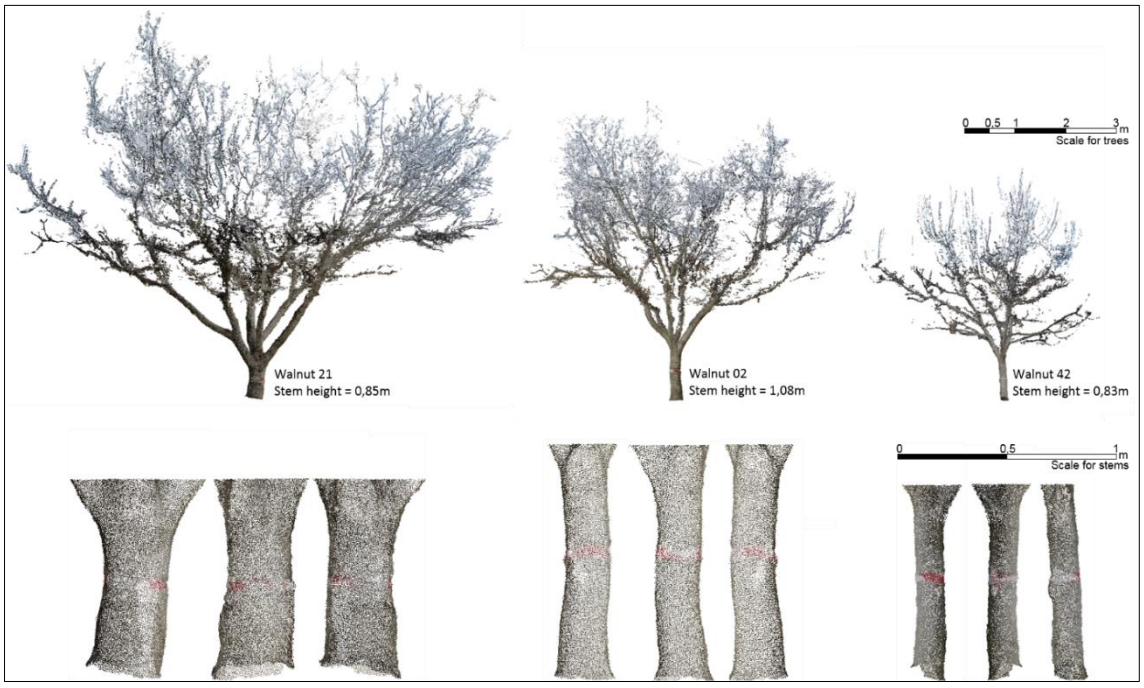

Fig. 4. Point clouds of three walnut, adult (left) middle age (center) and young (right). At the bottom of the figure, three views of the stem of each walnut area shown.

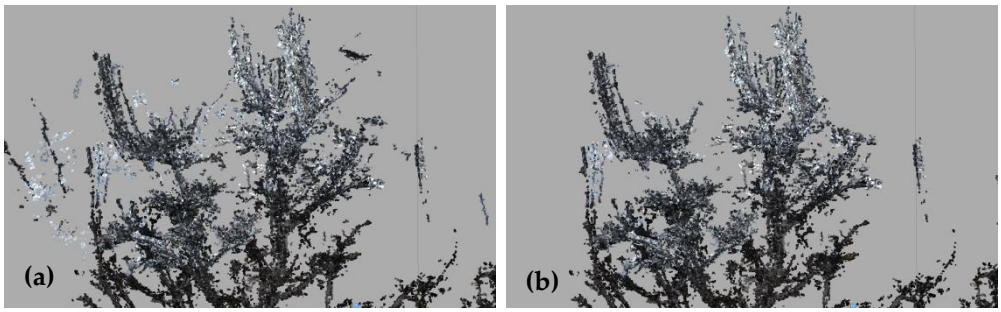

Fig. 5. Upper part of a walnut tree before (a) and after manual cleaning (b).

Extraction of walnut tree parameters from SfM point clouds

The walnut tree parameters were obtained processing the 3D point clouds for each tree using Cloudcompare (cross sections, subsample, statistical outlier removal,) and routines developed in Matlab (v. 7.11, the MathWorks Inc.; Natick, MA, 2010). Parameters such as total and crown height and stem diameter are extracted from attributes of the files using necessary specific tools. The difference in Z between the highest and lowest points of the 3D point cloud for each tree enables calculating total height values (Ht_{SfM}). After manually splitting the complete point cloud into crown and stem points (by identifying the base of the first branching of the stratum 1), the crown (Hc_{SfM}) and stem heights (Hs_{SfM}) can be obtained in the same way using the "min" and "max" functions of Matlab. The crown and stem points are then processed separately. For stem diameter (Ds_{SfM}) the average of the dimensions in X and Y directions of the 2 cm thick Z-section at a standard height of 60 cm was calculated (Fig. 6).

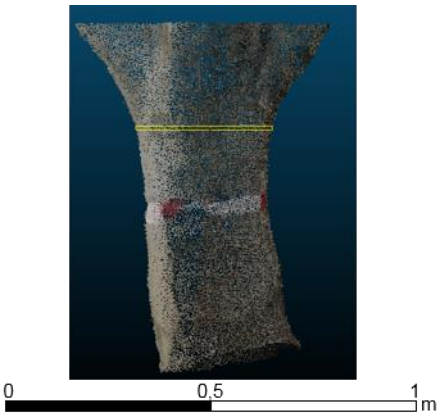

Fig. 6. Stem of an adult walnut tree and section used to measure its diameter (yellow section at 60 cm height).

Crown volumes and mean diameters have been calculated for each walnut using routines implemented in Matlab (distance and convhull functions) from crown and stem clouds. For volumes, two different algorithms were applied to compute the crown volume, as described in Fernández-Sarría et al. (2013) and Estornell et al. (2017) (Fig. 7). The first algorithm uses the convex hull function and it is applied to the file with the crown points with coordinates X, Y and Z for each tree. . The second method is a slight modification of the first one. The convex hull function is applied in each slice of 5 cm height in each crown. Every 5 cm slice creates a closed surface whose volumes are calculated and summed.

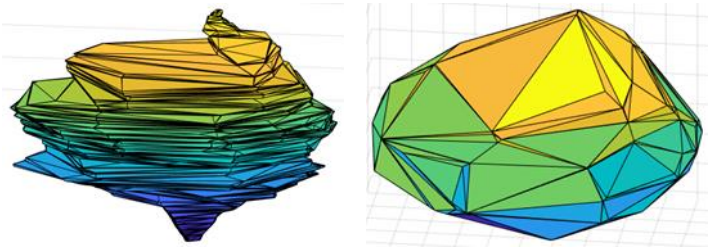

Fig. 7. Volumes over crown of an adult walnut tree. Convex hull global volume (left) and convex hull by slices (right).

The stem volume has been calculated by applying the Matlab routine described using (in this case) two algorithms: the first, by obtaining the convex hull formed by all the points of the stem; and the second, by applying it to each 5 cm section in the Z axis. To calculate the crown diameter (Dc_{SfM}), the following steps were applied using Matlab routines (more details in Fernández-Sarría et al. (2013)): the central coordinates of the upper part of the trunk cloud are used as a central point of the corresponding crown. For each crown point, the polar coordinates from the central point are calculated. A set of 72 circular sections, with five degrees of angle, are obtained in the XY plane projection of the crown. The longest of all the radii calculated within each section is selected and added to the longest radii of the symmetrical section, the section incremented 180 degree with respect to the specific section. This enables defining one diameter. The other 35 diameters are determined in the same way, and so obtaining a total of 36 values. Finally, the average of all the diameters was computed.

Estimation of parameters

A set of parameters derived from SfM data (Ds_{SfM}, Dc_{SfM}, Ht_{SfM}, Hc_{SfM}, Vs_{SfM}, VcSfM) were used as explanatory variables to estimate field parameters (Ds, Dc, Ht, Hc, Vs, Vc). Simple regression models were calculated obtaining the R^2, RMSE, and relative RMSE (RMSE%), calculated dividing the RMSE value by each parameter mean calculated from field data. For crown volume estimation, the two approaches described previously to retrieve crown volumes from 3D point clouds were analyzed (convex hull and convex hull by slices. It was then checked if the residues followed a normal distribution. For the stem and crown volume variables the condition was not met. Therefore, for these variables it is necessary to carry out the transformation into Napierian logarithms.

A leave-one-out-cross-validation method was applied to evaluate each regression model. The R^2, RMSE and RMSE% were obtained for the regression models and compared to those obtained from the

cross-validation technique. The residuals among field and cross-validation predicted parameters were also calculated and analyzed if they followed a normal distribution by applying a Shapiro-Wilk test ($p>0.05$).

Results

The parameters of walnut stems (diameter and volume) were estimated with considerable accuracy with R^2 values of 0.99 and 0.98 and RMSE values of 0.01 m (RMSE% = 6.44 %) and 0.12 (RMSE% = 3.32 %), respectively (Table 2). The simplest models (1 variable) were calculated to estimate all the structural parameters. For stem diameter estimation, the same parameter, but derived from 3D stem points, was selected showing a strong relationship between field vs. SfM parameter (Fig. 8). These results demonstrated the capability of the ground SfM technique to obtain stem diameters. For stem volume, the most accurate fit was obtained when convex hull algorithm by slices were used to model and calculate volume. The accurate results obtained for the stem parameters agree with the detail shown in the walnut stem in Fig. 6 where the 3D point cloud retrieved from SfM shows a defined structure for the walnut stem.

For crown parameters, the most accurate results were obtained for diameter and crown volume. In the first case, the values of R^2, RMSE, and RMSE % were 0.99, 0.26 m and 5.15 %, respectively. The selected variable to estimate this parameter was the crown diameter derived from the 3D crown point. This result shows a great degree of concordance with the crown diameter measured on the orthophoto. For crown volume, the calculated regression model showed a strong relationship between this parameter calculated from field data (using a paraboloid model) and the crown volume calculated by convex hull algorithm on the 3D point crown layer (the R^2 value being 0.99). Similar result was obtained (R^2=0.98) when the convex hull by slices algorithm was tested to compute crown volumes (results not shown). Less accuracy was obtained for crown height parameter with the values of R^2, RMSE and RMSE%, 0.90, 0.56 m and 13.3% respectively. Similar results were obtained for total height. For this parameter, an R^2 of 0.91 and RMSE of 0.56 m were obtained (RMSE% = 11%). For height parameters (total and crown), a more accurate fit was observed for small trees (Fig. 8). Overall, a strong correlation was also observed for these two parameters demonstrating the potential of the ground SfM technique to measure total and crown height.

Table 2 Parameters of the regression models. Estimated walnut parameters: stem diameter (Ds); stem volume (Vs); crown diameter (Dc); crown volume (Vc); crown height (Hc); total height (Ht). Independent variables derived from 3D point clouds using SfM method: stem diameter (DsSfM); stem volume calculated using convex hull algorithm by slices (Vs_{SfM}); crown diameter (Dc_{SfM}); crown volume calculated by convex hull algorithm (Vc_{SfM}); crown height (Hc_{SfM}); total height (Ht_{SfM}); determination coefficient for each model (R^2); root mean square error (RMSE); RMSE percentage compared to average field values for each parameter (RMSE %); cross validation determination coefficient (R^2cv); cross validation root mean square error (RMSEcv); statistic W of the Shapiro-Wilk test.

Parameter	Estimate	R^2	RMSE	RMSE (%)	R^2cv	RMSEcv	W Shapiro-Wilk	p-value
Constant	0.009	0.99	0.01	6.44	0.99	0.01	0.98	0.90
Ds_{SfM} (m)	0.954							
Model: $Ds = 0.009 + 0.954*Ds_{SfM}$								
Constant	0.324	0.98	0.12	3.32	0.98	0.13	0.98	0.90
$LnVs_{SfM}$ (dm^3)	0.952							
Model: $LnVs = 0.324 + 0.952*LnVs_{SfM}$								
Constant	0.307	0.99	0.26	5.15	0.99	0.27	0.97	0.54
Dc_{SfM} (m)	0.964							
Model: $Dc = 0.307 + 0.964*Dc_{SfM}$								
Constant	-0.612	0.99	0.17	1.52	0.98	0.13	0.98	0.09
$LnVc_{SfM}$ (m^3)	1.021							
Model: $LnVc = -0.612 + 1.021*LnVc_{SfM}$								
Constant	-0.066	0.90	0.56	13.33	0.89	0.59	0.97	0.33
Hc_{SfM} (m)	0.974							
Model: $Hc = -0.066 + 0.974*Hc_{SfM}$								
Constant	-0.118	0.91	0.56	10.96	0.91	0.59	0.97	0.37
Ht_{SfM} (m)	0.983							
Model: $Ht = -0.118 + 0.983*Ht_{SfM}$								

The comparisons of RMSE and R^2 values obtained for the regression models and cross validation techniques for each parameter were made to validate the results. In this line, similar values of RMSE - RMSEcv and R^2 - R^2cv were found for each parameter (Table 2). Furthermore, a linear relationship close to the 1:1 line was observed in the field data and cross validation predicted an R^2 value greater than 0.89 (Fig. 8). Residual distribution among field and cross validation predicted parameters for all the parameters were also analyzed. P-values in the Shapiro-Wilk test were higher than 0.05 – indicating that they were normally distributed (Table 2).

Fig. 8. shows the distribution of field vs. predicted values close to the 1:1 line in the analyzed variables. This figure contains the relationship between the predicted values (X-axis) when applying the leave-one-out cross validation technique and those observed in the field (Y-axis). The results of this graph and the values of the Shapiro-Wilk test (Table 2) enable justifying the validation of the models.

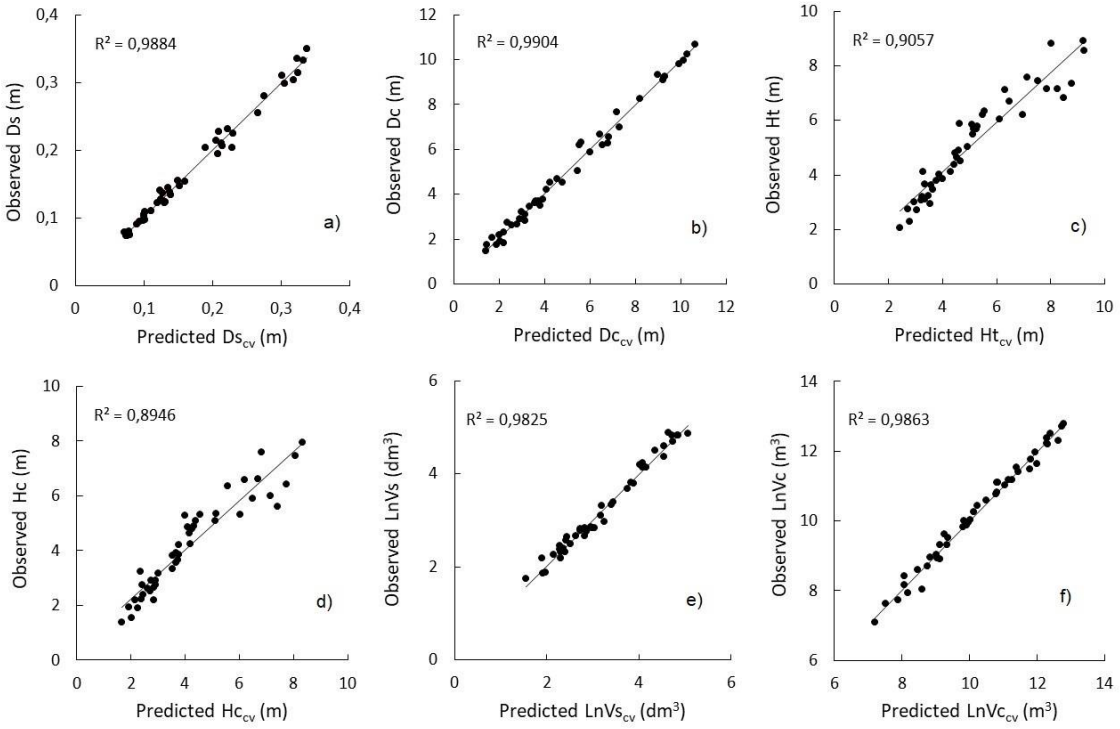

Fig 8. Scatterplot for each field and cross-validation predicted parameter (calculated from 3D point clouds using SfM method). Ds, diameter of the stem (a); Dc, diameter of the crown (b); Ht, total height (c); Hc, crown height (d); Vs, volume of the stem (e); Vc, volume of the crown (f).

Discussion

In this study, regression was performed to model and to establish the relationship of each observed and calculated parameter (Ht, Hc, Vc, Vs, Dc and Ds) obtaining R^2 values greater than 0.89 for all the models. These results indicate the capability of ground SfM for estimating the structural parameters of walnut trees. The same explicative variables (field data vs SfM method variables, Ds vs Ds_{SfM}; Vs vs Vs_{SfM}; Dc vs Dc_{SfM}; Vc vs Vc_{SfM}; Hc vs Hc_{SfM}; Ht vs Ht_{SfM}) were selected to estimate each parameter avoiding complex models whose geometrical and physical explanation could be not so evident (Table 2). The simplest models were calculated for each parameter (one explicative variable) by selecting the same parameter – but derived from 3D point clouds (Table 2). These parameters can be obtained using simpler traditional methods. However, computing a 3D tree model allows a better definition of their geometry and repeatability in the measurements. In addition, 3D point clouds enable characterizing other parts of the tree whose manual measurements in field are more complex and imprecise (crown diameter, crown area, diameter and length of the branches of stratum 1, etc.). On the other hand, some trees are large enough making that accurate measurements of height and crown diameter are difficult to obtain by traditional and simpler methods.

In terms of relative RMSE, it is interesting to note the results obtained for crown and stem diameters (5.15% and 6.44%, respectively) reveal a significant potential for this technique for measuring these parameters. For stem diameter, these results are in line with those reported by De Eugenio et al. (2018) for *Pinus pinaster* when applying ground SfM techniques. Similar results were also found for this parameter on forest trees registered with TLS systems (Heinzel et al. 2017; Pitkänen et al. 2019). These studies reported values of RMSE ranged from 0.7 cm to 2.1 cm. However, this technology, unlike ground SfM, is more time consuming and requires several stations to register completely each tree and the high cost of equipment limits its use (especially for small-medium plantation owners). The results obtained for this parameter could monitor growth and classify the trees according their sizes. The capability of ground SfM technique for estimating walnut crown diameters was also demonstrated in this study. This result was in accordance with findings reported in Estornell et al. (2017) for walnut trees. In this study, a TLS system was applied that obtained an RMSE value of 0.44 m. Both techniques enable modeling the crown of the tree in great detail while dealing with the irregularities found in crowns. In our study, the algorithm developed enabled computing 36 diameters from the 3D point cloud. In contrast, the measurement of the diameter by traditional methods presents some complexity, especially for leafless trees as shown in our

study. The border of the crown can be extracted in great detail from the 3D point clouds (Estornell et al. 2018). Previous studies have shown the relevance of crown diameter for estimating crown and pruning biomass in olive trees (Velázquez-Martí et al. 2011; Velázquez-Martí et al. 2014).

Lower values in terms of R^2 were found for height parameters (0.89-0.9), especially for large trees (Fig. 8). These results could be explained considering that the detection of the highest and terminal parts of the branches was difficult using terrestrial SfM algorithms. A mixture of reflections from sky and vegetation background can often occur when measuring high parts and this generates some noise and anomalous 3D points (Fig. 5). To our knowledge, no previous study has focused on estimating fruit tree parameters using terrestrial SfM. However, tree height parameters are estimated with other techniques. For instance, RMSE values in the range of 0.21 m and 0.43 m were reported for walnuts and olives using airborne LIDAR data, TLS and UAV systems (Díaz-Varela et al. 2015; Torres-Sánchez et al. 2015; López-Cortés et al. 2019). In our study, an RMSE of 0.56 m was obtained. To explain this higher value another issue should be considered. Walnut trees in our study were registered under leafless conditions and the small radiometric contrast with the background sky and the slight movement due to the low wind of the thinnest terminal branches makes the determination of tie points less accurate. More accurate results may be expected for leafy trees, when the high leaf coverage of the walnuts would make it possible to obtain true tie points adjusted to the crown envelope, and so generating a denser 3D point cloud that could enable defining the canopy with greater detail.

For crown volumes, significant relationships were found between paraboloid volumes, calculated from field data (crown height and crown diameter) and crown volumes computed from 3D point clouds. We would like to emphasize that this volume is not actual volume but geometrical volume. To know actual values of volume, it would be necessary to apply destructive methods or to determine the volume of each branch by other measuring methods. Two procedures were tested (convex hull and convex hull by slices). The estimation of crown volume by applying the convex hull method is more accurate than using a 3D shape model such as a paraboloid based on traditional measurements. Differences between these methods can even be more relevant for irregularly shapes and leafless crowns as those considered in our study. Several studies reported the potential of the crown volume parameter in precision agriculture for adjusting spray volume (Miranda-Fuentes et al. 2016) and calculating the leaf area index (Arnó et al. 2013). In addition, these results could be applied for estimating crown biomass based on a widely accepted biophysical relationship between crown volume and crown biomass. Allometric equations based on field

data for estimating this parameter are not common in agriculture, and these values need to be obtained from destructive samples. Therefore, the results obtained could be applied to estimate crown biomass in an indirect way using information retrieved of 3D models developed in our study. Another aspect to be mentioned is that the photographs were captured for trees under leafless conditions (early February). This situation offers advantages and disadvantages. The main advantage of the absence of leaves is that the solid structure of the trunk and the thicker branches can be modeled with greater detail than with thinner and more terminal branches, which are complex to model with this technique. Trees in this stage offer a better approximation to the amount of wood biomass. For trees with leaves, crown solid volumes can be defined by the enveloped 3D shape that could be also used to estimate in an indirect way crown biomass. For stem volume, an accurate regression model was also reported. Walnut stems show a approximate cylindrical geometry that was identified clearly from the 3D point clouds. For crown and stem volumes, it should be noted that R^2 values represent the percentage of variation explained by crown and stem volumes computed by the 3D point cloud, respectively. These variables were previously transformed to meet linearity model assumptions (for instance normality of the residuals). Therefore, these results were reported in the linearized space, and not in the original scale. These results should be analyzed with caution.

Conclusions

Several walnut parameters were derived successfully and accurately in our study such as crown diameters, crown and total height and crown and stem volume using terrestrial automated photogrammetry (ground-based SfM technique). These parameters are of interest for the management of fruit plantations as reported in the article. The technique used in this study was SfM method applied on images taken by a standard digital camera, not requiring specific instruments (laser scanner, aerial LiDAR sensors, GNSS devices) or specialized users to capture the data. This technique constitutes a low-cost observation technique unlike other capture systems. For these, specific and more expensive devices are used, and other auxiliary devices where the measurement equipment are installed and which often require more logistics. In addition, unlike ground SfM methods, these observation systems require a higher level of user specialization.

Previous studies applied this terrestrial approach to determine different parameters of forest trees. Despite this, it is necessary to explore the suitability of this technique on fruit trees with crowns, branches and stems of smaller dimensions. For these reasons, testing the potential of this low-cost technology on

these trees is of interest. The possibilities of modeling both the canopy and the stem in three dimensions are interesting for many applications such as pruning, quantification of wood biomass, phytosanitary treatments, CO_2 sequestration and for estimating biofuel production.

Although promising results were obtained for the estimated parameters (in terms of R^2 and RMSE), there are some aspects that could be improved in our study. As reported, difficulties to model the highest and smallest branches were observed (some duplications, incomplete branches due to occlusions, erroneous 3D points), and lower accuracy was found for the total height and the crown height compared to the rest of parameters. Despite these limitations, we obtained accurate values for R^2, RMSE and RMSE %. Images were taken in leafless conditions making more challenging the use of this method for determining these parameters. However, this observation condition has advantages as reported in the article (accurate definition of the stem and more information of tree branches). For leafy trees a better definition of the upper parts of the canopy could be obtained by detecting a greater number of tie points automatically in the photogrammetric processes. These acquisition advantages require to be analyzed in further studies to improve the results obtained in this study.

References

Arnó J, Vallès JM, Llorens J, Sanz R, Masip J, Palacín J, Rosell-Polo JR (2013) Leaf area index estimation in vineyards using a ground-based LiDAR scanner. Precis Agric 14(3): 290-306. https://doi.org/10.1007/s11119-012-9295-0.

Arnó J, Masip J, Rosell-Polo JR (2015) Influence of the scanned side of the row in terrestrial laser sensor applications in vineyards: practical consequences. Precis Agric 16(2):119-128. https://doi.org/10.1007/s11119-014-9364-7.

Auat Cheein F, Guivant J, Sanz R, Escolà A, Yandún F, Torres-Torriti M, Rosell-Polo, JR (2015) Real-time approaches for characterization of fully and partially scanned canopies in groves. COMPAG 118, 361–371. https://doi.org/10.1016/j.compag.2015.09.017.

Bork EW, Su JG (2007) Integrating LiDAR data and multispectral imagery for enhanced classification of rangeland vegetation: A meta analysis. Remote Sens Environ 111:11–24. https://doi.org/10.1016/j.rse.2007.03.011.

Brede B, Calders K, Lau A, Raumonen P, Bartholomeus H, Herold M, Kooistra L (2019) Non-destructivetree volume estimation through quantitative structure modelling: comparing UAV laser scanning with terrestrial LIDAR. Remote Sens Environ 233: p. 111355. https://doi.org/10.1016/j.rse.2019.111355.

Cadena C, Carlone L, Carrillo H, Latif Y, Scaramuzza D, Neira J, Reid I, Leonard JJ (2016) Past, Present, and Future of Simultaneous Localization and Mapping: Toward the Robust-Perception Age. IEEE Trans Robot 32:1309–1332. https://doi.org/10.1109/tro.2016. 2624754.

Calders K, Newnham G, Burt A, Murphy S, Raumonen P, Herold M, Culvenor D, Avitabile V, Disney M, Armston J, Kaasalainen M (2015) Nondestructive estimates of above-ground biomass using terrestrial laser scanning. Methods Ecol Evol 6: 198-208. https://doi.org/10.1111/2041-210X.12301.

Chang A, Jung J, Maeda MM, Landivar J (2017) Crop height monitoring with digital imagery from Unmanned Aerial System (UAS), COMPAG 141:232–237. https://doi.org/10.1016/j.compag.2017.07.008.

Cunliffe AM, Brazier RE, Anderson K (2016) Ultra-fine grain landscape-scale quantification of dryland vegetation structure with drone-acquired structure-from-motion photogrammetry, Remote Sens Environ 183:129–143. https://doi.org/10.1016/j.rse.2016.05.019.

Dalla A, Rex F, Almeida D, Sanquetta C, Silva C, Moura M, Wilkinson B et al (2020) Measuring Individual Tree Diameter and Height Using GatorEyeHigh-Density UAV-Lidar in an Integrated Crop-Livestock-Forest System. Remote Sens 12:863. https://doi.org//10.3390/rs12050863.

De Eugenio A, Fernández-Landa A, Merino-de-Miguel S (2018) 3D models from terrestrial photogrammetry in the estimation of forest inventory variables. Revista de Teledetección 51:113–124. https://doi.org/10.4995/raet.2018.9174.

Díaz-Varela R, de la Rosa R, León L, Zarco-Tejada P (2015) High-Resolution airborne uav imagery to assess olive tree crown parameters using 3D photo reconstruction: Application in breeding trials. Remote Sens 7(4):4213–4232. https://doi.org/10.3390/rs70404213.

Dong J, Burnham JG, Boots B, Rains G, Dellaert F (2017) 4D crop monitoring: Spatio-temporal reconstruction for agriculture. In Proceedings of the IEEE International Conference on Robotics and Automation (ICRA), Singapore, pp. 3878–3885. https://doi.org/ 10.1109/ICRA.2017.7989447.

Ehlert D, Heisig M, Adamek R (2010) Suitability of a laser rangefinder to characterize winter wheat. Precis Agric 11:650–663.

Escolà A, Martínez-Casasnovas JA, Rufat J, Arnó J, Arbonés A, Sebé F, Pascual M, Gregorio E, Rosell-Polo JR (2017) Mobile terrestrial laser scanner applications in precision fruticulture/horticulture and tools to extract information from canopy point clouds. Precis Agric 18:111–132. https://doi.org/10.1007/s11119-016-9474-5.

Estornell J, Ruiz LA, Velázquez-Martí B, López-Cortés I, Salazar D, Fernández-Sarría A (2015) Estimation of pruning biomass of olive trees using airborne discrete-return LiDAR data. Biomass Bioenergy 81:315-321. https://doi.org/10.1016/j.biombioe.2015.07.015.

Estornell J, Velázquez-Martí A, Fernández-Sarría A, López-Cortés I, Martí-Gavilá J, Salazar D (2017) Estimation of structural attributes of walnut trees based on terrestrial laser scanning. Revista de Teledetección .0(48), 67-76. https://doi.org/10.4995/raet.2017.7429

Estornell J, Velázquez-Martí B, Fernández-Sarría A, Martí J (2018) Lidar methods for measurement of trees in urban forests. J Appl Remote Sens 12(4):046009. https://doi.org/10.1117/1.JRS.12.046009.

Fernández-Sarría A, Martínez L, Velázquez-Martí B, Sajdak M, Estornell J, Recio JA (2013) Different methodologies for calculating crown volumes of Platanus hispanica trees using terrestrial laser scanner and a comparison with classical dendrometric measurements. COMPAG 90:176-185.

Fernández-Sarría A, López-Cortés I, Estornell J, Velázquez-Martí B, Salazar D (2019) Estimating residual biomass of olive tree crops using terrestrial laser scanning. Int J Appl Earth Obs Geoinf 75:163-170. https://doi.org/10.1016/j.jag.2018.10.019.

Gené-Mola J, Gregorio López E, Auat Cheein FA, Guevara J, Llorens Calveras J, Sanz Cortiella R, Rosell Polo JR (2020) Fruit detection, yield prediction and canopy geometric characterization using LiDAR with forced air flow. COMPAG 168:105121. https://doi.org/10.1016/j.compag.2019.105121.

Gil E, Arnó J, Llorens J, Sanz R, Llop J, Rosell-Polo JR, Gallart M, Escolà A (2014) Advanced Technologies for the Improvement of Spray Application Techniques in Spanish Viticulture: An Overview. Sensors 14: 691–708. https://doi.org/10.3390/s140100691.

Goesele M, Snavely N, Seitz SM, Curless B, Hoppe H (2007) Multi-view stereo for community photo collections. In Proceedings of the11th International Conference on Computer Vision, Rio de Janeiro, Brazil pp. 1-8. https://doi.org/ 10.1109/ICCV.2007.4408933.

Gómez-Candón D, De Castro AI, López-Granados F (2014) Assessing the accuracy of mosaics from unmanned aerial vehicle (UAV) imagery for precision agriculture purposes in wheat. Precis Agric 15(1):44–56. https://doi.org/10.1007/s11119-013-9335-4.

Gonzalez de Tanago J, Lau A, Bartholomeus H, Herold M, Avitabile V, Raumonen P, Martius C, Goodman R, Disney M, Manuri S et al (2018) Estimation of above ground biomass of large tropical trees with terrestrial LiDAR. Methods Ecol Evol 9(2):223-234. https://doi.org/10.1111/2041-210X.12904.

Guerra-Hernández J, Cosenza DN, Estraviz Rodriguez LC, Silva M, Tomé M, Díaz-Varela RA, González-Ferreiro E (2018) Comparison of ALS- and UAV(SfM)-derived high-density point clouds for individual tree detection in Eucalyptus plantations, Int J Remote Sens 39(15–16):5211–5235, https://doi.org/10.1080/01431161.2018.1486519.

Hadas E, Borkowski A, Estornell J, Tymkow P (2017) Automatic estimation of olive tree dendrometric parameters based on airborne laser scanning data using alpha-shape and principal component analysis. GIsci Remote Sens 54(6):898–917.https://doi.org/10.1080/15481603.2017.1351148

Hargreaves GH (1994) Defining and Using Reference Evapotranspiration. J Irrig Drain Eng 120(6). https://doi.org//10.1061/(ASCE)0733-9437(1994)120:6(1132).

Heinzel J, Huber MO (2017) Tree stem diameter estimation from volumetric TLS image data. Remote Sens 9, 614, https://doi.org/10.3390/rs9060614.

Jay S, Rabatel G, Hadoux X, Moura D, Gorretta N (2015) In-field crop row phenotyping from 3D modeling performed using Structure from Motion. COMPAG 110:70-77.

Jenkins J, Chojnacky D, Heath L, Birdsey R (2004) Comprehensive Database of Diameter-Based Biomass Regressions for North American Tree Species; United States Forest Service, Northeastern Research Station: New Town Square, PS, USA, p.45.

Jiménez-Brenes FM, López-Granados F, Castro AI, Torres-Sánchez J, Serrano N, Peña JM (2017) Quantifying pruning impacts on olive tree architecture and annual canopy growth by using UAV-based 3D modelling. Plant Methods 13:1–15. https://doi.org/10.1186/s13007-017-0205-3.

Kankare I, Räty M, Yu X, Holopainen M, Vastaranta M, Kantola T, Hyyppä J, Hyyppä H, Alho P, Viitala R (2013) Single tree biomass modelling using airborne laser scanning, ISPRS J Photogramm Remote Sens 85:66-73. https://doi.org/10.1016/j.isprsjprs.2013.08.008.

Lefsky MA, Cohen WB, Parker GG, Harding DJ (2002) LiDAR remote sensing for ecosystem studies. Bioscience 52, 19–30.

Liang X, Kankare V, Hyyppä J, Wang Y, Kukko A, Haggrén H, Yu X, Kaartinen H, Jaakola A, Guan F, Holopainen M, Vastaranta M (2016) Terrestrial laser scanning in forest inventories. ISPRS J Photogramm Remote Sens 115, 63-77.

López-Cortés I, Martí-Gavilá J, Estornell J, Fernández-Sarría A (2019) Comparación de parámetros de olivos a partir de UAV y datos LiDAR aéreos. In Proceedings of XVIII Congreso de la Asociación Española de Teledetección, Valladolid, Spain, 24-27 September 2019; pp. 439-442.

Lowe D (2004) Distinctive Image Features from Scale-Invariant Keypoints. Int J Comput Vis 60(2), 91–110, https://doi.org/10.1023/B:VISI.0000029664.99615.94.

Maltamo M, Räty J, Korhonen L, Kotivuori E, Kukkonen M, Peltola H, Kangas J, Packalen P (2020) Prediction of forest canopy fuel parameters in managed boreal forests using multispectral and unispectral airborne laser scanning data and aerial images. Eur J Remote Sens. https://doi.org/10.1080/22797254.2020.1816142.

Miao Y, Mulla DJ, Randall GW, Vetsch, JA, Vintila R (2009) Combining chlorophyll meter readings and high spatial resolution remote sensing images for in-season site-specific nitrogen management of corn. Prec Agric 10, 45–62, https://doi.org/10.1007/s11119-008-9091-z.

Miller J, Morgenroth J, Gomez C (2015) 3D modelling of individual trees using a handheld camera: Accuracy of height, diameter and volume estimates. Urban For Urban Green 14(4), 932-940. https://doi.org/10.1016/j.ufug.2015.09.001.

Ministerio de Agricultura, Pesca y Alimentación (2019) Encuesta sobre superficies y rendimientos cultivos (ESYRCE). Encuesta de marco de áreas de España. 178 pp. Available online:

https://www.mapa.gob.es/es/estadistica/temas/estadisticas-agrarias/agricultura/esyrce/(accessed on 15 September 2021).

Miranda-Fuentes A, Llorens J, Rodriguez-Lizana A, Cuenca A, Gil E, Blanco-Roldán GL, Gil-Ribes JA (2016) Assessing the optimal liquid volume to be sprayed on isolated olive trees according to their canopy volumes. STOTEN 568:296-305. https://doi.org/10.1016/j.scitotenv. 2016.06.013.

Moorthy I, Miller JR, Jimenez Berni JA, Zarco-Tejada P, Hu B, Chen J (2011) Field characterization of olive (*Olea europaea* L.) tree crown architecture using terrestrial laser scanning data. Agric For Meteorol 151(2): 204–214, https://doi.org/10.1016/j.agrformet. 2010.10. 005

Neuenschwander A, Pitts K (2019) The ATL08 land and vegetation product for the ICESat-2 Mission. Remote Sens Environ 221:247-259, https://doi.org//10.1016/j.rse.2018.11.005.

Palacín J, Pallejà T, Tresanchez M, Sanz R, Llorens J, Ribes-Dasi M, Masip J, Arnó J, Escolà A, Rosell JR (2007) Real-Time Tree-Foliage Surface Estimation Using a Ground Laser Scanner. IEEE Trans Instrum Meas 56(4):1377–1383. https://doi.org/10.1109/TIM.2007. 900126.

Pierzchala M, Giguère P, Astrup R (2018) Mapping forests using an unmanned ground vehicle with 3D LiDAR and graph-slam, COMPAG 145:pp. 217-225. https://doi.org/10.1016/j.compag.2017. 12.034.

Pitkänen TP, Raumonen P, Kangas A (2019) Measuring stem diameters with TLS in boreal forests complementary fitting procedure. ISPRS J Photogramm Remote Sens 147:294-306, https://doi.org/10.1016/j.isprsjprs.2018.11.027.

Popescu SC (2007) Estimating biomass of individual pine trees using airborne LiDAR. Biomass Bioenergy 31(9):646–655. https://doi.org/10.1016/j.biombioe.2007.06.022.

Sanz R, Llorens J, Escolà A, Arnó J, Planas S, Román C, Rosell-Polo JR (2018) LiDAR and non-LiDAR-based canopy parameters to estimate the leaf area in fruit trees and vineyard. Agric For Meteorol 260-261: 229–239. https://doi.org/10.1016/j.agrformet.2018.06.017.

Schlaegel B (1984) Green Ash Volume and Weight Tables. US Department of Agriculture, Forest Service, Southern Forest Experiment Station: New Orleans, LA, USA.

Sheridan RD, Popescu SC, Gatziolis D, Morgan CLS, Ku NW (2015) Modeling forest aboveground biomass and volume using airborne LiDAR metrics and forest inventory and analysis data in the Pacific Northwest. Remote Sens 7:229–255. https://doi.org/10.3390/rs70100229.

Snavely N, Seitz SM, Szeliski R (2008) Modeling the world from Internet photo collections. Int J Comput Vis 80(2):189–210. https://doi.org/10.1007/s11263-007-0107-3.

Stereńczak K, Kraszewski B, Mielcarek M, Piasecka N, Lisiewicz M, Heurich M (2020) Mapping individual trees with airborne laser scanning data in an European lowland forest using a selfcalibration algorithm. Int J Appl Earth Obs Geoinf 93:102191, https://doi.org/10.1016/j.jag.2020.102191.

Tagarakis AC, Koundouras S, Fountas S. Gemtos T (2018) Evaluation of the use of LIDAR laser scanner to map pruning wood in vineyards and its potential for management zones delineation. Precis. Agric. 19:334–347. https://doi.org/10.1007/s11119-017-9519-4.

Torres-Sánchez J, López-Granados F, Serrano N, Arquero O, Peña JM (2015) High-Throughput 3-D Monitoring of Agricultural-Tree Plantations with Unmanned Aerial Vehicle (UAV) Technology. PLoS ONE 10(6):e0130479. https://doi.org/10.1371/journal.pone.0130479.

Torres-Sánchez J, de Castro A, Peña JM, Jiménez-Brenes FM, Arquero O, Lovera M et al (2018) Mapping the 3D structure of almond trees using UAV acquired photogrammetric point clouds and object-based image analysis. Biosyst Eng 176:172–184.https://doi.org/10.1016/j.biosystemseng.2018.10.018.

Valbuena MA, Santamaría J, Sanz F (2016) Estimation of diameter and height of individual trees for Pinus sylvestris L. based on the individualising of crowns using airborne LiDAR and the National Forest Inventory data. For Syst 25(1):e046. http://dx.doi.org/10.5424/fs/2016251-05790.

Van der Zande V, Hoet W, Jonckheere I, van Aardt J, Coppin P (2006) Influence of measurement set-up of ground-based LiDAR for derivation of tree structure. Agric For Meteorol 141(2–4): 147–160. https://doi.org/10.1016/j.agrformet.2006.09.007.

Velázquez-Martí B, Fernández-González E, López-Cortes I, Salazar-Hernández DM (2011) Quantification of the residual biomass obtained from pruning of trees in Mediterranean olive groves. Biomass Bioenergy 35(2):3208–3217. https://doi.org/10.1016/j.biombioe.2011.04.042.

Velázquez-Martí B, López-Cortés I, Salazar DM (2014) Dendrometric analysis of olive trees for wood biomass quantification in Mediterranean orchards. Agroforestry Systems 88(5):755-765. http://dx.doi.org/10.1007/s10457-014-9718-1.

Walklate PJ, Cross JV, Richardson GM, Murray RA, Baker DE (2002) Comparison of different spray volume deposition models using LIDAR measurements of apple orchards. Biosyst Eng 82(3):253–267.

Wallace L, Lucieer A, Malenovský Z, Turner D, Vopenka P (2016) Assessment of Forest Structure Using Two UAV Techniques: A Comparison of Airborne Laser Scanning and Structure from Motion (SfM) Point Clouds. Forests 7: 62. https://doi.org/10.3390/f7030062.

Wang X, Cheng X, Gong P, Huang H, Li Z, Li X (2011) Earth science applications of ICESat/GLAS: a review. Int J Remote Sens 32:23, 8837-8864.

Wieser M, Mandlburger G, Hollaus M, Otepka J, Glira P, Pfeifer N (2017) A Case Study of UAS Borne Laser Scanning for Measurement of Tree Stem Diameter. Remote Sens 9:1154. https://doi.org//10.3390/rs9111154.

Xie Q, Dash J, Huete A, Jiang A, Yin G, Ding Y, Peng D, Hall CC, Brown L, Shi Y et al (2019) Retrieval of crop biophysical parameters from Sentinel-2 remote sensing imagery. Int J Appl Earth Obs Geoinf 80:187–195. https://doi.org/10.1016/j.jag.2019.04.019.

Xing, D., Bergeron, J. C., Solarik, K. A., Tomm, B., Macdonald, S. E., Spence, J. R., He, F. (2019). Challenges in estimating forest biomass: use of allometric equations for three boreal tree species. Canadian Journal of Forest Research, 49(12), 1613-1622.

Zarco-Tejada PJ, Diaz-Varela R, Angileri V, Loudjani P (2014) Tree height quantification using very high resolution imagery acquired from an unmanned aerial vehicle (UAV) and automatic 3D photo-reconstruction methods. Eur J Agron 255: 89–99.

Zhang Z, Cao L, She G (2017) Estimating Forest Structural Parameters Using Canopy Metrics Derived from Airborne LiDAR Data in Subtropical Forests. Remote Sens 9:940. https://doi.org/10.3390/rs9090940.